THE JOURNAL OF PHYSICAL CHEMISTRY B

Article

pubs.acs.org/JPCB

Heat Capacities and Glass Transitions of Ion Gels

Osamu Yamamuro,*[,†] Takenori Someya,[†] Maiko Kofu,[†] Takeshi Ueki,[‡] Kazuhide Ueno,[‡] and Masayoshi Watanabe[‡]

[†]Neutron Science Laboratory, Institute for Solid State Physics, University of Tokyo, 5-1-5 Kashiwanoha, Kashiwa, Chiba 277-8581, Japan

[‡]Department of Chemistry and Biotechnology, Yokohama National University, 79-5 Tokiwadai, Hodogaya-ku, Yokohama, Kanagawa 240-8501, Japan

ABSTRACT: We have investigated thermodynamic properties of ion gels consisting of a PMMA [poly(methyl methacrylate)] network and EMITFSI [1-ethyl-3-methylimidazolium bis-(trifluoromethanesulfonyl)imide] ionic liquid by means of an adiabatic calorimeter. The heat capacity data were measured in the temperature range between 5 and 375 K for 7 samples with x = 0 (pure PMMA), 0.10, 0.18, 0.27, 0.48, 0.65, and 1.0 (pure ionic liquid) where x is a mole fraction of EMITFSI. These data revealed that two broad but distinct glass transitions appeared in the low x region. The upper glass transition is mainly due to the freezing of the PMMA motion, while the lower one is due to the ionic liquid. The upper glass transition temperature T_g drastically decreased with increasing x, reflecting a large plasticization effect observed in mechanical experiments. The x dependence of the T_gs and the excess heat capacities gave new physical insight to the interaction between polymer and ionic liquid in ion gels.

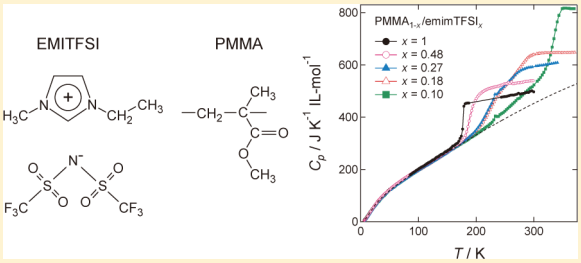

INTRODUCTION

"Ion gels", which were first developed by the Watanabe group,[1,2] are some sort of polymer gels with ionic liquids (ILs) as solvents. They chose PMMA (poly(methyl methacrylate)) as the polymer and EMITFSI (1-ethyl-3-methylimidazolium bis-(trifluoromethanesulfonyl)imide) as the ionic liquid (see Figure 1). The ion gels possess properties of both ionic liquids and gels;

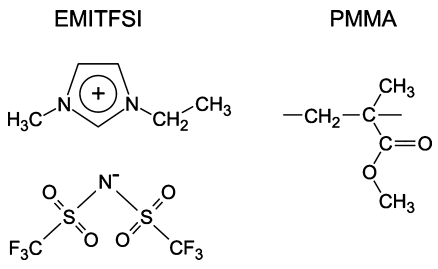

Figure 1. Molecular/ionic structures of components of PMMA/EMITFSI ion gel.

the ion gels form transparent, soft, and strong membranes with high ionic conductivity, negligible vapor pressure, and thermal stability.[1−3] These properties attract a great deal of attention in applications for various electrochemical devices, actuators, and so on. Other than the PMMA/EMITFSI system, a new series of ion gels, composed of ionic liquid and block polymer, has recently been synthesized.[4−6] The combination of ionic liquid and polymers enables the design of new materials with high ionic conductivity and easy portability. In the work by Seki et al.,[1] the glass transition temperature T_g was determined by a differential scanning calorimeter (DSC) and the Vogel−Fulcher temperature T_0[7,8] was determined by extrapolating the $\sigma-T$ curve to σ = 0, where σ is ionic conductivity and T is temperature. T_g and T_0 tend to separate off with decreasing the mole fraction x of EMITFSI as if there are "two glass transitions". They argued that the decoupling feature, for the motions of polymer and ionic liquid, is apparent at lower x. It should be emphasized that the decoupled dynamics are not usual phenomena in hydrogels and low-molecular binary solutions. In fact, observation of a single T_g is typically considered as a criterion for establishing miscibility of two components in binary systems. Recently, the existence of two T_gs has been observed in some miscible polymer blends,[9−13] but the mechanism of this phenomenon is still under discussion. Another important aspect in the ion gel system is the "plasticization" of polymer due to the ionic liquid. The dynamic mechanical analysis (DMA)[2] indicated that the upper T_g which decreases drastically with increasing x corresponds to the stiffness of the gel. The mechanism of the plasticization is interesting not only for the application use but also to investigate the interaction between the polymer and the ionic liquid. The purpose of the present study is to investigate the coupling−decoupling and plasticization phenomena described above from the thermodynamic point of view. We used an adiabatic calorimeter which provides absolute values of heat capacity with very high resolution and are suitable for the relaxation phenomena such as glass transitions. It is expected to find two glass transitions in the PMMA/EMITFSI system.

Received: March 30, 2012
Revised: July 25, 2012
Published: August 14, 2012

   dx.doi.org/10.1021/jp3030655 | J. Phys. Chem. B 2012, 116, 10935−10940

EXPERIMENTAL SECTION

Sample Preparation. 2,2-Azobisisobutyronitrile (AIBN) was from Sigma-Aldrich. All other chemical reagents were from Wako Pure Chemical Industries, Ltd., Japan. AIBN was recrystallized from methanol prior to use. Methyl methacrylate (MMA) and ethylene glycol dimethacrylate (EGDMA) were purified by distillation under reduced pressure over CaH_2. Other chemical reagents were used as received without further purification. 1-Ethyl-3-methylimidazolium bis-(trifluoromethanesulfonyl)imide (EMITFSI) was synthesized and characterized according to the reported procedures.[14] MMA monomer, EGDMA (2 mol % based on MMA) as a cross-linker, and AIBN (1 mol % based on MMA) as an initiator were dissolved in EMITFSI. The reaction mixtures were degassed using a N_2 purge for 20 min. The radical polymerization was carried out at 60 °C for 24 h. A further heat treatment at 140 °C for 30 min was conducted in order to complete polymerization. The resulting ion gels were flexible, transparent, and self-standing films. In addition, PMMA (bulk) films, which did not contain any IL, were also prepared as a reference material following the polymerization technique identical to that of the ion gel. The compositions of the samples measured in the present experiment are $x = 0$ (pure PMMA), 0.10, 0.18, 0.27, 0.48, 0.65, and 1.0 (pure ionic liquid) where x is a mole fraction of EMITFSI.

Heat Capacity Measurement. The heat capacity measurements were performed with an in-house-built adiabatic calorimeter in the temperature range from 5 to 340 K.[15] Only for pure EMITFSI ($x = 1.0$) which crystallizes readily on cooling, a top-loading adiabatic calorimeter[16] was used to avoid crystallization by rapid cooling; the sample cell was immersed in liquid nitrogen before it was loaded into the cryostat. The cooling rate is roughly estimated to be 200 K min^{-1}. The samples were loaded into the copper cell with helium gas which facilitates thermal equilibration inside the cell. The masses of the samples with $x = 0$, 0.10, 0.18, 0.27, 0.48, 0.65, and 1.0 are 1.227 15, 1.213 70, 1.401 53, 0.821 02, 1.309 06, 2.303 48, and 2.4988 g, respectively. All the measurements were carried out using a standard intermittent heating method, i.e., repetition of equilibration and energizing intervals. The temperature increment for each measurement was 0.3 K around 5 K and increased with increasing temperature to reach 2.5 at 200 K. The temperature increment was reduced to smaller than 1 K in the regions of the glass transition and fusion. The accuracy of the heat capacity measurement was better than 1% at $T < 10$ K, 0.5% at 10 K < T < 30 K, and 0.1% at $T > 30$ K for both calorimeters.

RESULTS AND DISCUSSION

Heat Capacity. Figure 2 shows the heat capacity of pure EMITFSI. The closed circles denote the data for the glassy and liquid sequence and the open ones for the crystalline state. A glass transition with a large heat capacity jump appeared at 177 K. On the course of the measurement of the supercooled liquids, a crystallization with a large exothermic effect occurred at 185 K. After the sample was annealed at 250 K to obtain complete crystalline state, the heat capacity of the crystalline sample was measured from 80 K. A large endothermic effect due to the fusion appeared around 270 K. The fusion temperature was determined to be (271 ± 0.5) K from the measurement with temperature increment of ca. 1.0 K. The enthalpy and entropy of fusion were (21.07 ± 0.02) kJ mol^{-1} and (77.8 ± 0.1) J K^{-1} mol^{-1}, respectively. The origin of a small peak around 240 K is unknown; it can be a crystalline phase transition or an eutectic melting owing to some impurity.

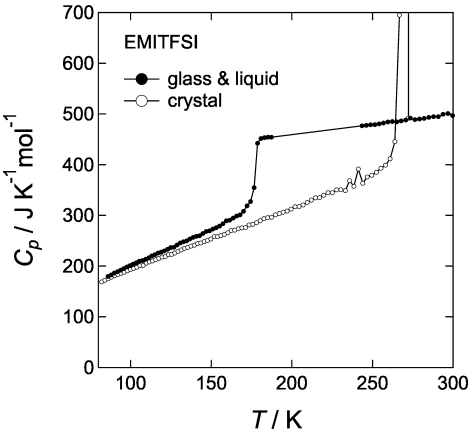

Figure 2. Heat capacities of bulk EMITFSI.

Figure 3 shows the heat capacities of $PMMA_{1-x}/EMITFSI_x$ with $x = 0$, 0.10, 0.18, 0.27, and 0.48. Glass transitions appeared in the samples except pure PMMA; the T_g of pure PMMA ($x = 0$) was reported to be 378 K[17] that is higher than the high-temperature limit of our calorimeter. The shapes of the glass transitions are broader than that of the pure EMITFSI. For the samples with $x = 0.18$ and 0.27, the heat capacity increases in two steps at the glass transitions. The glass transition temperatures and the magnitudes of the heat capacity jumps will be determined precisely later. We have also measured the heat capacities of the sample with $x = 0.65$ but do not plot them in Figure 3. This is because we found that the sample was not in a gel state but just a mixture of PMMA and EMITFSI. At $x = 0.65$, the content of PMMA is not enough to form network structure to confine ionic liquid.

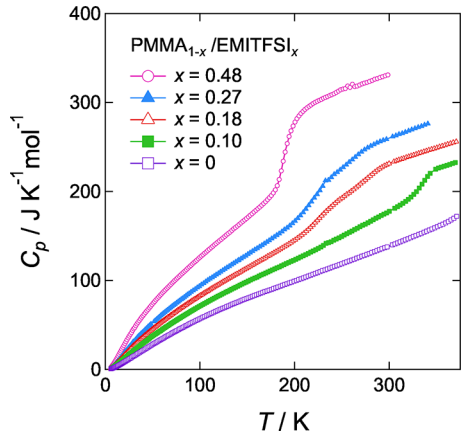

Figure 3. Heat capacities of ion gels $PMMA_{1-x}/EMITFSI_x$.

Temperature Drift Rate. One of the useful pieces of information obtained only by adiabatic calorimetry is the temperature drift rate as a function of temperature. In the adiabatic condition, temperature should be constant if the sample is in an equilibrium state. However, if the sample is in nonequilibrium conditions such as in glass transitions, irreversible phase transitions, etc., one can observe a spontaneous exothermic or endothermic effect during an equilibration period after heating.

dx.doi.org/10.1021/jp3030655 | J. Phys. Chem. B 2012, 116, 10935−10940

Figure 4 shows the temperature drift rates of the pure EMITFSI and the PMMA/EMITFSI ion gels. The glass

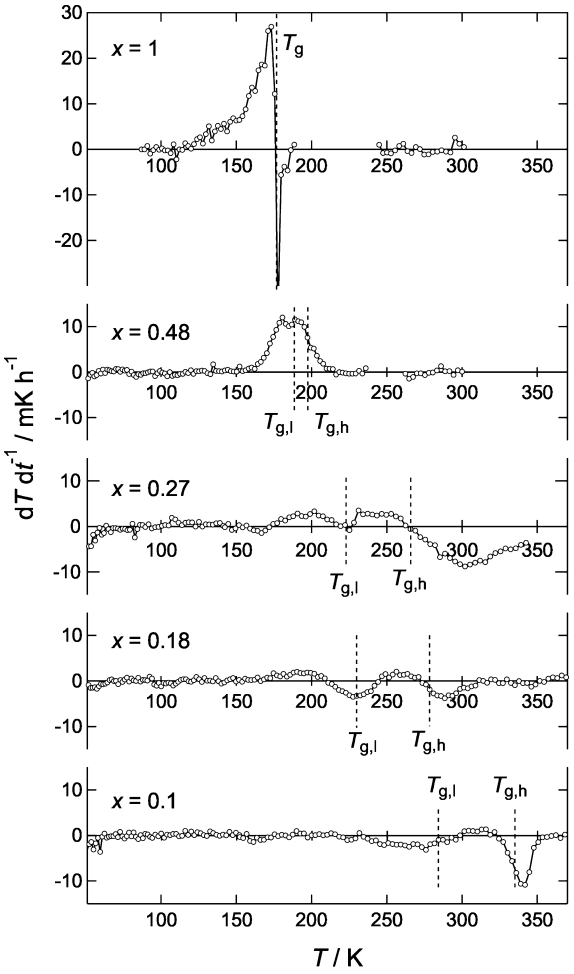

Figure 4. Spontaneous temperature drift rates during equilibration periods of heat capacity measurements of ion gels $PMMA_{1-x}/EMITFSI_x$. Glass transition temperatures determined from ΔC_p are shown by dashed lines (see text for details).

transition temperatures determined in the following section are shown by dashed lines. In pure EMITFSI, an exothermic effect followed by an endothermic one appeared at 120−180 K. The glass transition temperature, which is usually defined as the temperature where the heat capacity increases most steeply, corresponds to the temperature where the drift rate changes from positive to negative. This is a characteristic drift rate at the glass transition and its mechanism has been clarified by Suga and Seki.[18,19]

In the ion gels, there are clearly two exothermic-to-endothermic effects, namely two glass transitions. The endothermic drift is not clear due to an endothermic−exothermic overlapping effect in the sample with $x = 0.48$. The exothermic effect is not clear in the sample with $x = 0.1$ and the T_g of the lower glass transition does not correspond to the temperature where the drift rate changes from positive to negative. This may be because the glass transition becomes broader at this mole fraction as described later.

Separation of Two Glass Transitions. We have subtracted the heat capacity of glassy PMMA from the total heat capacities of the ion gels. Figure 5 gives the remaining heat capacities

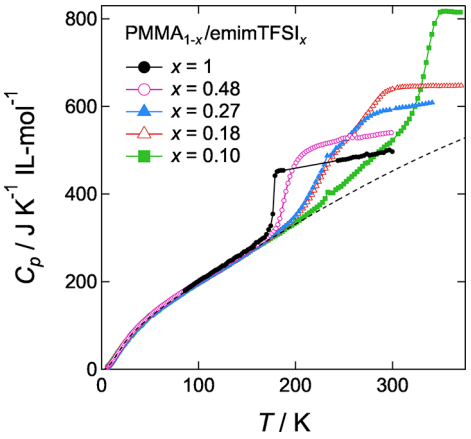

Figure 5. Heat capacities of ion gels $PMMA_{1-x}/EMITFSI_x$ subtracted heat capacities of glassy PMMA. The dashed curve represents the vibrational heat capacity. See text for the details.

plotted as the values per mole of EMITFSI. The heat capacity of pure EMITFSI is also plotted for comparison. Surprisingly, all of the heat capacities coincide with each other below T_g, indicating that the additivity of the heat capacities between EMITFSI and PMMA is valid below T_g; the additivity above T_g will be discussed later.

The heat capacity of the glassy EMITFSI is fitted by the combination of the Debye and Einstein functions as shown by a dashed curve in Figure 5. The details of the fitting have been reported elsewhere.[20] Figure 6 shows the excess heat capacities

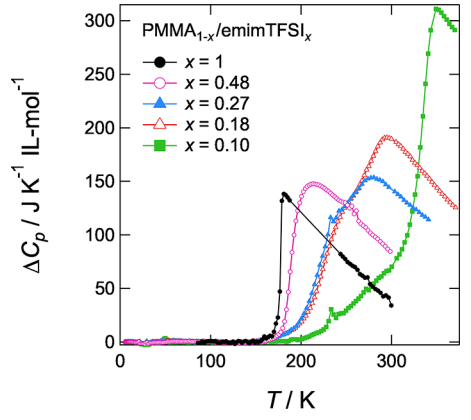

Figure 6. Excess (configurational) heat capacities of ion gels $PMMA_{1-x}/EMITFSI_x$.

ΔC_p above T_g obtained by subtracting the dashed curve from the heat capacities shown in Figure 5. The existence of two glass transitions are clearly shown even for the sample with $x = 0.48$; the lower T_g is not easy to be noted in Figure 3. The small anomalies around $T = 230$ K are due to the fusion of remaining EGDMA, a cross-linker for gelation.

The ΔC_p data are fitted by the sum of two sigmoid functions:

$$\Delta C_p = \Delta C_{p,l} + \Delta C_{p,h} = \frac{L_l[1 - a(T - T_{g,l})]}{1 + \exp[-r_l(T - T_{g,l})]} + \frac{L_h[1 - a(T - T_{g,h})]}{1 + \exp[-r_h(T - T_{g,h})]} \quad (1)$$

where L is the magnitude of the C_p jump at T_g, r is a parameter reflecting the steepness of the glass transition, and a is a

dx.doi.org/10.1021/jp3030655 | J. Phys. Chem. B 2012, 116, 10935−10940

parameter corresponding to the gradient of ΔC_p above T_g. The subscripts l and h denote the lower and higher glass transitions, respectively. The parameter a is assumed to be common both for the lower and higher glass transitions to reduce the number of the fitting parameters. Of course, the fitting for pure EMITFSI was performed using one sigmoid function. The ΔC_p data are fitted well as shown in Figure 7, where the results of the fitting are shown for the samples with $x = 0.1$ and 0.27; similar results were obtained also for the samples with $x = 0.18$ and 0.48.

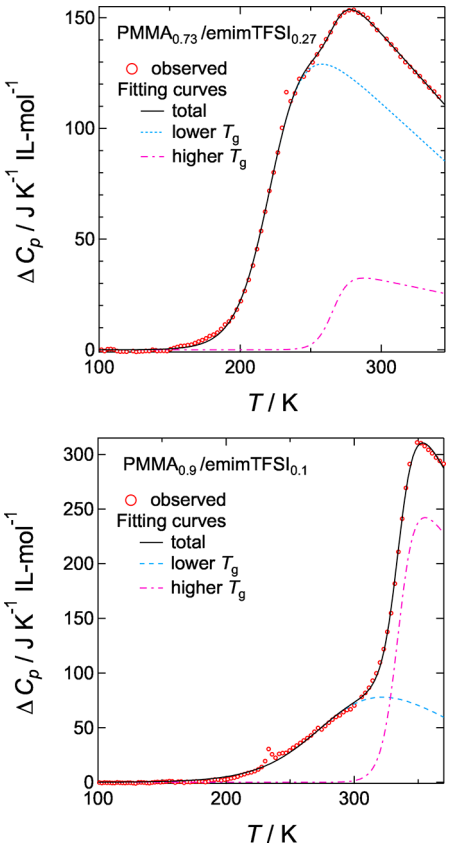

Figure 7. Fittings of the excess heat capacities of ion gels $PMMA_{1-x}$/$EMITFSI_x$. See text for details.

Composition Dependence of Glass Transition Temperatures. The T_gs determined in the analysis described above are plotted against the mole fraction of ionic liquid x in Figure 8. The bars with plotted symbols are not error bars (the errors of the fitting to eq 1) but $\pm r/2$ in eq 1 corresponding to the widths of the glass transitions. In the temperature region $T_g \pm r/2$, ΔC_p changes from ca. $0.1L$ to $0.9L$. $T_{g,h}$, mainly corresponding to the motion of PMMA, steeply decreases with increase of x. On the other hand, $T_{g,l}$, mainly corresponding to the motion of EMITFSI, gradually decreases with increase of x. It is also remarkable that the width of $T_{g,l}$ becomes larger with decreasing x.

Mok et al.[21] have reported two glass transitions in their DSC (differential scanning calorimetry) work on polymer solutions (not gels) of PMMA and EMITFSI. Their T_gs are also plotted in Figure 8. It is of interest that our T_gs and the mole fraction dependence of T_gs are close to those of Mok's even though one is for the ion gels and the other is for the polymer solutions. This may be because the glass transitions are dominated by the local

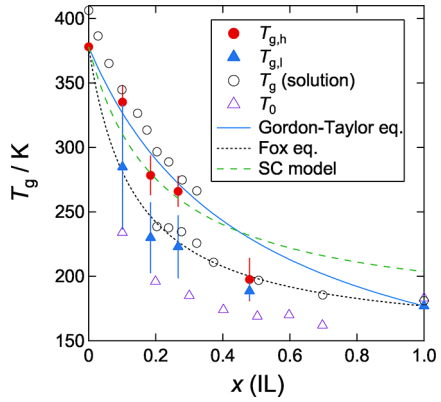

Figure 8. Glass transition temperatures T_g of $PMMA_{1-x}$/$EMITFSI_x$ as a function of the mole fraction x of ionic liquid. T_g for the solutions of PMMA and EMITFSI[21] and the Vogel–Fulcher temperatures T_0 determined from the conductivity data[1] are also plotted. Curves are the values calculated from the models described in the text.

structure that is common for the ion gels and the polymer solutions.

There are two well-known equations to represent the mole fraction dependence of T_gs in polymer–polymer compatible systems and polymer–solvent solution systems. One is Gordon–Taylor equation[22]

$$T_g = v_A T_{g,A} + v_B T_{g,B} \quad (2)$$

and the other is Fox equation[23]

$$\frac{1}{T_g} = \frac{w_A}{T_{g,A}} + \frac{w_B}{T_{g,B}} \quad (3)$$

where v_A and v_B ($v_A + v_B = 1$) are volume fractions and w_A and w_B ($w_A + w_B = 1$) are weight fractions; volume fractions are sometimes used for both equations. Roughly speaking, eq 2 is based on a weighted average of macroscopic properties related to glass transitions (e.g., viscosity), while eq 3 of microscopic properties related to glass transitions (e.g., activation energy). It is suggestive that the $T_{g,h}$s are reproduced well by eq 2 while the $T_{g,l}$s by eq 3.

Another important model to reproduce the mole fraction dependence of T_gs in polymer blends is the self-concentration model developed by Lodge and MacLeish.[24] This model is based on the concept that the local concentration ϕ_{eff} of a monomer of type A polymer is larger than the average concentration ϕ owing to the chain connectivity; a monomer is bound to other monomers in the same chain. ϕ_{eff} is given by

$$\phi_{eff} = \phi_s + (1 - \phi_s)\phi \quad (4)$$

where ϕ_s is termed the "self-concentration". ϕ_s is evaluated as a concentration of a monomer averaged in a volume V defined by the Kuhn length l_k

$$\phi_s = \frac{l_k M}{k l \rho N_A V} \quad (5)$$

where M is the repeat unit molar mass, k is the number of backbone bonds, l is the average length of backbone bonds, and ρ is the density. By assuming $V = l_k^3$ (spherical and cylindrical volumes are also possible) and inputing the following values for PMMA at 413 K,[24] $l_k = 13.8$ Å, $M = 100$ g/mol, $k = 2$, $l = 1.53$ Å, and $\rho = 1.13$ g/cm^3, ϕ_s is calculated to be 0.25. The curve calculated from eq 3 with ϕ_{eff} instead of w is shown in Figure 8.

dx.doi.org/10.1021/jp3030655 | J. Phys. Chem. B 2012, 116, 10935–10940

This curve well reproduces the mole fraction dependence of $T_{g,h}$ up to $x = 0.27$ but deviates significantly at higher x.

From the results described above, it is confirmed that $T_{g,h}$ is dominated by the motion of PMMA and its x dependence directly reflects the plasticization of PMMA caused by adding the ionic liquid. On the other hand, $T_{g,l}$ mainly corresponds to the motion of EMITFSI. This is justified by the fact that similar x dependence is obtained for the T_0 determined from the ionic conductivity.[1] The width of the glass transitions indicates that $T_{g,l}$ is affected more strongly by the distribution of local structures than $T_{g,h}$. It should be recalled that the $T_{g,h}$ is reproduced well by the Gordon−Taylor equation while the $T_{g,l}$ by the Fox equation. These results are consistent with the well-known fact that the space scale of polymer dynamics, probably of the order of 10 Å, is longer than that of solvent molecules. In other words, PMMA is affected by the averaged interaction of several EMITFSI ions around the polymer chain, while EMITFSI by the interaction of neighboring PMMA with distribution of EMITFSI−PMMA distances. This is supported also by the fact that the self-concentration model, incorporating the interaction within the volume defined by the Kuhn length (13.8 Å), is valid for the mole fraction dependence of $T_{g,h}$ in the low-IL concentration region.

Excess Heat Capacities and Their Additivity. Figure 9 shows the ΔC_ps determined by the fitting to eq 1 (symbols) and

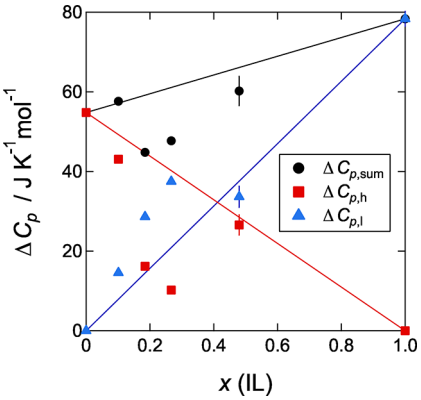

Figure 9. Excess heat capacities $\Delta C_{p,l}$ and $\Delta C_{p,h}$ at 250 K for the lower and high glass transitions, respectively. The sum of them $\Delta C_{p,sum}$ is also plotted. Lines represent the weighted averages of the excess heat capacities of the pure PMMA and EMITFSI.

the simple weighted average of each pure component (lines). The ΔC_p for the higher glass transition, the lower glass transition, and their summation are plotted against the mole fraction x. The ΔC_ps were calculated at 250 K where the extrapolation is most reliable for both higher and lower glass transitions. Since we could not measure the C_p above the T_g (=378 K) of pure PMMA, the following equation

$$\Delta C_p = 96.83 - 0.1672T - 1.9024T^{-2} (190\text{K} < T < 550\text{K}) \quad (6)$$

based on the previous work[17] is used.

It is clearly shown that the ΔC_p of the lower glass transition is larger than the weighted average while that of the higher glass transition is smaller than the weighted average. This tendency increases with increasing x and disappears at $x = 0.48$. This effect can be explained by assuming that the configurational motion of some part of PMMA (e.g., ester group) is involved in the lower glass transition which is mainly due to the freezing of EMITFSI; both are frozen almost together at $x = 0.48$.

In most of compatible binary systems, the additivity of the heat capacity is valid; i.e., the heat capacity is reproduced well by adding the heat capacity of each component. However, the sum of ΔC_p of each component of the ion gel is smaller than the experimental value at $x = 0.18$ and 0.27. This may be because some local structures to reduce configurational excitation are formed at these compositions. At $x = 0.48$, the additivity of the excess heat capacity comes back. Detailed structural analyses are desirable for further investigation of the interaction between the polymer and the ionic liquid.

CONCLUSION

The present work has revealed that two broad but distinct glass transitions appeared in the low x region. The upper glass transition is mainly due to the freezing of the PMMA motion, while the lower one is due to the ionic liquid. The upper glass transition temperature $T_{g,h}$ drastically decreased with increasing x, reflecting a large plasticization effect observed in the mechanical experiments. The lower glass transition temperature $T_{g,l}$ reflects the ionic conductivity of the ion gels. The mole fraction dependence (Gordon−Taylor or Fox) and the width of the glass transitions indicate that the motion of the polymer has a longer space scale than the motion of the ionic liquids. The consideration on the additivity of the heat capacity suggests that some local structure between PMMA and EMITFSI is formed at intermediate concentration range ($x = 0.18$ and 0.27).

AUTHOR INFORMATION

Corresponding Author

*E-mail: yamamuro@issp.u-tokyo.ac.jp.

Notes

The authors declare no competing financial interest.

ACKNOWLEDGMENTS

This work is financially supported by the Grant-in-Aid for Scientific Research on Priority Area No. 17073004, MEXT, Japan.

REFERENCES

(1) Seki, S.; Susan, M. A. B. H.; Kaneko, T.; Tokuda, H.; Noda, A.; Watanabe, M. *J. Phys. Chem. B* **2005**, *109*, 3886−3892.
(2) Susan, M. A. B. H.; Kaneko, T.; Noda, A.; Watanabe, M. *J. Am. Chem. Soc.* **2005**, *127*, 4976−4983.
(3) Ueki, T.; Watanabe, M. *Macromolecules* **2008**, *41*, 3739−3749.
(4) He, Y.; Boswell, P. G.; Buhlmann, P.; Lodge, T. P. *J. Phys. Chem. B* **2007**, *111*, 4645−4652.
(5) He, Y.; Lodge, T. P. *Macromolecules* **2008**, *41*, 167−174.
(6) Lodge, T. P. *Science* **2008**, *321*, 50−51.
(7) Vogel, H. *Phys. Z.* **1922**, *22*, 645−646.
(8) Fulcher, G. S. *J. Am. Ceram. Soc.* **1925**, *8*, 339−355.
(9) Savin, D. A.; Larson, A. M.; Lodge, T. P. *J. Polym. Sci., Part B: Polym. Phys.* **2004**, *42*, 1155−1163.
(10) Lodge, T. P.; Wood, E. R.; Haley, J. C. *J. Polym. Sci., Part B: Polym. Phys.* **2005**, *44*, 756−763.
(11) Sakaguchi, T.; Taniguchi, N.; Urakawa, O.; Adachi, K. *Macromolecules* **2005**, *38*, 422−428.
(12) Miwa, Y.; Usami, K.; Yamamoto, K.; Sakaguchi, M.; Sakai, M.; Shimada, S. *Macromolecules* **2005**, *38*, 2355−2361.
(13) Gaikwad, A. N.; Wood, E. R.; Ngai, T.; Lodge, T. P. *Macromolecules* **2008**, *41*, 2502−2508.
(14) Bonhote, P.; Dias, A. -P.; Papageorgiou, N.; Kalyanasundaram, K.; Gratzel, M. *Inorg. Chem.* **1996**, *35*, 1168−1178.

(15) Yamamuro, O.; Oguni, M.; Matsuo, T.; Suga, H. *Bull. Chem. Soc. Jpn.* **1987**, *60*, 1269−1275.
(16) Tsukushi, I.; Yamamuro, O.; Sadanami, K.; Nishizawa, M.; Matsuo, T.; Takeda, K. *Rev. Sci. Instrum.* **1998**, *69*, 179−184.
(17) Gaur, U.; Lau, S. F.; Wunderlich, B. B.; Wunderlich, B. *J. Phys. Chem. Ref. Data* **1982**, *11*, 1065−1089.
(18) Suga, H.; Seki, S. *J. Non-Cryst. Solids* **1974**, *16*, 171−194.
(19) Suga, H.; Seki, S. *Faraday Discuss. Chem. Soc.* **1980**, *69*, 221−240.
(20) Yamamuro, O.; Tsukushi, I.; Lindqvist, A.; Takahara, S.; Ishikawa, M.; Matsuo, T. *J. Phys. Chem. B* **1998**, *102*, 1605−1609.
(21) Mok, M. M.; Liu, X.; Bai, Z.; Lei, Y.; Lodge, T. P. *Macromolecules* **2011**, *44*, 1016−1025.
(22) Gordon, M.; Taylor, J. S. *J. Appl. Chem.* **1952**, *2*, 493−500.
(23) Fox, T. G. *Bull. Am. Phys. Soc.* **1956**, *1*, 123.
(24) Lodge, T. P.; McLeish, T. C. B. *Macromolecules* **2000**, *33*, 5278−5284.